

Nanocrystallization in Al-based Metallic Glasses

Dmitri V. Louzguine-Luzgin¹, Guoqiang Xie² and Akihisa Inoue^{1,2}

¹ WPI Advanced Institute for Materials Research, Tohoku University, Aoba-Ku, Sendai 980-8577, Japan

² Institute for Materials Research, Tohoku University, Aoba-Ku, Sendai 980-8577, Japan

Al-RE-Ni-Co glassy alloys (RE – rare earth), exhibit ultra-high strength up to about 1.2 GPa which increases further up to about 1.5 GPa on their nanocrystallization. Here we summarize a large set of the experimental data related to the phase transformations leading to the formation of a nanostructure in Al-based glassy alloys. The crystallization of these alloys takes place either by nucleation and growth (N&G) in $\text{Al}_{85}\text{RE}_8\text{Ni}_5\text{Co}_2$ alloys or by growth of so-called “pre-existing” nuclei and nanoparticles in $\text{Al}_{85}\text{Y}_8\text{Ni}_{4.3}\text{Co}_2\text{Cu}_{1.2}$ and $\text{Al}_{85}\text{Y}_{6.4}\text{Ni}_5\text{Co}_2\text{Pd}_{2.4}$ alloys. The crystallization behavior of Al-RE-Ni-Co glassy alloys can be classified as follows: If an alloy does not show glass-transition at T_g on heating prior to crystallization and exhibits a N&G transformation mechanism then it forms intermetallic compound(s) (IM) or IM+nanoscale α -Al. If an alloy contains pre-existing nuclei then it does not show glass-transition and forms primary nanoscale α -Al. If an alloy shows glass-transition on heating and exhibits a N&G transformation mechanism then it forms nanoscale Al above T_g and IM+Al or IM below T_g . The kinetics of these phase transformations is also studied. We also found that the supercooled liquid region in the Al-based alloys strongly depends upon electronegativity of the RE metal. Contrary to crystallization on heating, no intermetallic compounds but only a very small volume fraction of α -Al nano particles was formed in the cold-rolled $\text{Al}_{85}\text{Y}_8\text{Ni}_5\text{Co}_2$ and $\text{Al}_{85}\text{Nd}_8\text{Ni}_5\text{Co}_2$ alloys, while $\text{Al}_{85}\text{Gd}_8\text{Ni}_5\text{Co}_2$ and $\text{Al}_{85}\text{Mm}_8\text{Ni}_5\text{Co}_2$ samples remain amorphous. Direct observation of micro-strain and dislocations quenched in α -Al nanoparticles with a size below 7 nm in a $\text{Al}_{85}\text{Y}_4\text{Ni}_5\text{Co}_2\text{Pd}_4$ alloy is also provided.

Keywords: *metallic glasses, nanocrystallization, phase transformation, kinetics.*

1. Introduction

An amorphous single phase has been formed over a wide composition range in binary Al-RE (RE-rare earth metal) [1] and ternary Al-RE-TM (TM-transition metals) [2] system alloys produced by rapid solidification techniques. Amorphous alloys in the ternary Al-Y-Ni system were found to possess high strength and good bending ductility (can be bent through 180° without fracture) [3,4]. The addition of Co [5] improved the glass-forming ability of the alloys and increased the mechanical strength which exceeded 1200 MPa. A newly discovered $(\text{Al}_{0.84}\text{Y}_{0.09}\text{Ni}_{0.05}\text{Co}_{0.02})_{95}\text{Sc}_5$ amorphous alloy has an ultra-high tensile fracture strength exceeding 1500 MPa which surpasses those for all the other Al-based fully crystalline and amorphous alloys reported up to date [6]. Quaternary $\text{Al}_{85}\text{Y}_8\text{Ni}_5\text{Co}_2$ alloy shows one of the widest supercooled liquid region on heating among Al-based metallic glasses (all alloy compositions are given in nominal atomic percents (at.%) [7].

Nanostructured alloys are readily obtained on primary devitrification of glasses with a long-range diffusion controlled growth [8]. Fine precipitates of the Al solid solution (α -Al), almost pure Al, formed by devitrification of the glassy matrix were found to increase tensile strength of the alloys without reduction of bending ductility [9]. Strengthening effect was also observed in case of nanoscale precipitates of quasicrystalline particles [10]. In amorphous materials the deformation is concentrated in the shear bands of maximum shear stress which maintain about 45 degrees with the load (tensile or compressive) direction. The width of the shear band in Al alloys is about 10-20 nm. The increase in strength by the dispersion of nanoscale fcc-Al particles in the amorphous matrix is

hence the nanoscale Al particles can act as barriers against the shear deformation of amorphous matrix.

Crystallization behaviour of various Al-Y-Ni and Al-Y-Ni-Co alloys has been also intensively studied and at definite compositions formation of the α -Al was observed in the primary stage [11,12]. In fact many other Al-based glassy and amorphous alloys [13,14] also exhibited formation of the nanoscale α -Al particles in the primary crystallization stage [15,16]. Crystallization of other quaternary and quinary alloys was also investigated [17,18]. Primary α -Al particles were also formed in Al-Ni-Ce alloy in which segregation of the RE metal with low diffusivity in Al on the (α -Al/amorphous phase) interface [19] is considered to be one of the most important reasons for the low growth rate of α -Al.

It has also been found that deformation of some Al-RE-TM amorphous alloys at room temperature causes precipitation of α -Al particles of 7-10 nm in diameter within the shear bands on bending [20] or nano-indentation [21]. Under tensile test they were found on the fracture surface only [22].

In the present paper we present and review our research data on crystallization of Al-based alloys.

2. Experimental Procedure

Ingots of the Al-RE-TM1-TM2 alloys (TM denotes transition metal) were prepared by arc-melting in an argon atmosphere the mixtures of pure metals having at least 99.9 mass% purity. From these alloys, ribbon samples of about 0.02 mm in thickness were prepared by rapid solidification of the melt on a single copper roller. The structure of the ribbon samples was examined by X-ray diffractometry using the monochromatic $\text{CuK}\alpha$ radiation. Transmission electron microscopy (TEM) investigation was carried out by using a microscope operating at 200 kV and equipped with an energy dispersive X-ray spectrometer (EDX). The phase transformation temperatures and heat effects during transformations were studied by differential scanning calorimetry (DSC) and by differential isothermal calorimetry (DIC).

3. Results and Discussion

3.1 Crystallization of Al-based metallic glasses above and below T_g .

An important difference in the devitrification pathways of Al based non-crystalline alloys is connected with the state of the matrix phase prior to crystallization. It can be amorphous, glassy or supercooled liquid. One can arbitrary define an alloy being “amorphous” if it crystallizes directly and does not transform to a supercooled liquid before crystallization. In general, glassy alloys exhibiting the supercooled liquid region on heating prior to crystallization have higher glass-forming ability compared to amorphous alloys. We found that on heating glassy and amorphous $\text{Al}_{85}\text{RE}_8\text{Ni}_5\text{Co}_2$ alloys, namely, $\text{Al}_{85}\text{Y}_8\text{Ni}_5\text{Co}_2$, $\text{Al}_{85}\text{Y}_{8-x}\text{Nd}_x\text{Ni}_5\text{Co}_2$ and $\text{Al}_{85}\text{Gd}_8\text{Ni}_5\text{Co}_2$ and others exhibit different devitrification behavior above and below glass-transition temperature (T_g) (Fig. 1 and Table. 1).

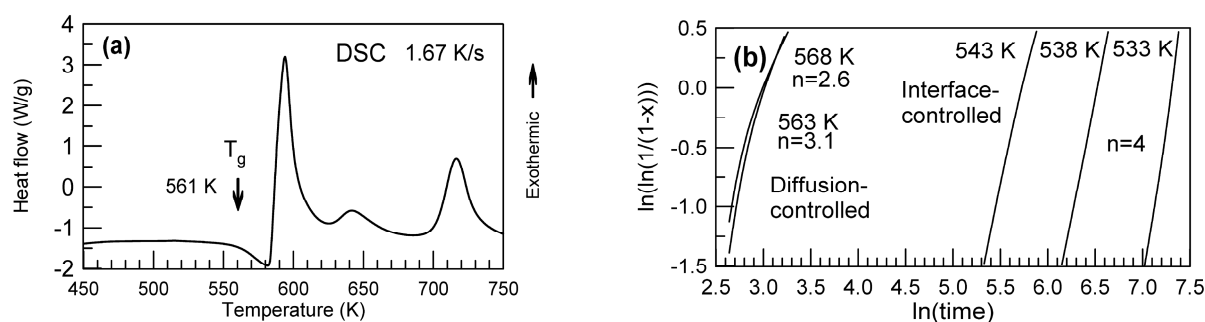


Fig. 1. (a) DSC curve of $\text{Al}_{85}\text{Ni}_5\text{Y}_4\text{Nd}_4\text{Co}_2$ alloy obtained at a heating rate of 1.67 K/s, (b) Avrami plot for isothermal calorimetry data at different temperatures above and below T_g of about 561 K.

Table 1. Crystallization behavior of Al₈₅Ni₅Y₄Nd₄Co₂ alloy near the glass-transition region.

Temperature, K	Transformation type	Avrami exponent, n	Phases formed
533, 538, 543	Interface-controlled growth	4	α-Al+IM
563	Diffusion -controlled growth	3.1	α-Al+traces of IM
568		2.6	α-Al

Below T_g most of glassy alloys showed a single-stage transformation obeying the kinetic law ($x(t)=1-\exp[-Kt^n]$) [23] for the fraction transformed (x) as a function of time (t) with Avrami exponent (n) close to 4 (K is a constant) while n values on the primary crystallization of nanoscale α -Al in the Al₈₅Dy₈Ni₅Co₂, Al₈₅Y₈Ni₅Co₂, Al₈₅Y₄Nd₄Ni₅Co₂ and other metallic glasses above T_g varies not only with temperature but with time as well exhibiting non-steady state nucleation (Fig. 1(b)). α -Al nanocrystals only are formed on rapid enough heating and annealing above T_g . Amorphous Al₈₅La₈Ni₅Co₂, Al₈₅Nd₈Ni₅Co₂, and Al₈₅Mm₈Ni₅Co₂ alloys which crystallize directly and do not exhibit glass-transition on heating did not show any temperature dependence of their crystallization products. One should also point out that from general viewpoint low-temperature phase transformation (Metallic glass→IM phase+ α -Al) looks similar to an irregular eutectic type. However, common interface between two phases is required for coupling growth. Al and IM phase in many cases do not have common interface and likely nucleate separately from the glassy phase.

Based on our findings, the crystallization of various Al-based glassy and amorphous alloys can be described by one of the three following types of mechanisms: 1. If an alloy does not show T_g on heating prior to devitrification/crystallization and exhibits nucleation and growth transformation mechanism then it forms intermetallic compound(s) (IM) or IM+nanoscale fcc-Al from the amorphous matrix. 2. If an alloy does not show glass-transition on heating prior to devitrification and has pre-existing nuclei then it forms nanoscale primary fcc-Al. 3. If an alloy shows glass-transition on heating and exhibits nucleation and growth transformation mechanism then it forms nanoscale fcc-Al above T_g and IM+ α -Al or IM below T_g .

These crystallization mechanisms can be associated with a new topological empirical criterion which was proposed for the design of multicomponent Al-rich amorphous alloys [24]. Such a criterion, is similar to the topological instability criterion [25], (λ parameter), as the ratio of solute atoms (r_i) of concentration C_i to Al atomic radius (r_{Al}) defined by equation:

$$\lambda = \sum_{i=B}^Z C_i \cdot \left| \frac{r_i^3}{r_{Al}^3} - 1 \right| \quad (1)$$

The λ parameter can successfully predict the thermal behavior for a given Al-based alloy composition, being able to indicate compositions which exhibit supercooled liquid region ($\lambda>0.1$), nanocrystalline behavior ($\lambda<0.1$) or alloys with an intermediate, nano-glassy behavior, where nanocrystallization is preceded by a supercooled liquid region ($\lambda\approx 0.1$). Following the concept of the effect of the electronegativity difference [26] on the width of the supercooled liquid region in Al-based metallic glasses two Al-based glassy alloys: Al₈₅Y₆Ni₅Co₂Zr₂ and Al₈₄Y₆Ni₄Co₂Sc₄ with the largest supercooled liquid region known so far of about 50 K were created [27]. Al₈₄Y₆Ni₄Co₂Sc₄ alloy has an empirical topological criterion $\lambda=0.1$ while the Al₈₅Y₆Ni₅Co₂Zr₂ one has $\lambda=0.091$, which is also not far from 0.1.

One could suppose that under-critical nuclei size medium range-order zones and clusters are formed upon relaxation as the relaxed sample still exhibits nucleation and growth transformation at T_x compared to Al-based marginal glass-formers which exhibit no glass-transition but just growth of pre-existing nuclei which were likely formed on cooling of the supercooled liquid above T_g when atomic mobility is still high. The results of this work also indicate that within a certain composition range the lower electronegativity difference leading to more entirely metallic type of bonding among the constituent elements is necessary to improve the stability of the supercooled liquid in Al-based glassy alloys. Another factor influencing the glass-forming ability and stability of a supercooled

liquid and a glass is atomic size ratio. It is well-established that the higher atomic size ratio, in general, leads to the higher glass-forming ability and stability of the glass [28]. In the present case we observe different behavior, i.e., the addition of Zr, an element with smaller Zr/Al atomic size ratio (ASR) of 1.12 substituting Y having $ASR_{Y/Al}$ of 1.27 (according to Goldschmidt atomic radii [29]) increases both T_g and T_x . Moreover, much worse correlation has been obtained between Goldschmidt atomic radii of the alloying RE metals in $Al_{85}RE_8Ni_5Co_2$ with ΔT_x (coefficient of determination (R^2) for the least-squares fitting with linear function was 0.63) compared to that with electronegativity of the constituent RE ($R^2=0.99$).

3.2 Deformation-induced crystallization in Al-based glassy alloys

The deformation-induced crystallization was studied in the glassy $Al_{85}Y_8Ni_5Co_2$ and $Al_{85}Gd_8Ni_5Co_2$ as well as amorphous $Al_{85}Nd_8Ni_5Co_2$ and $Al_{85}Mm_8Ni_5Co_2$ ribbon samples subjected to cold rolling with 33 % reduction in thickness [30]. The glassy $Al_{85}Y_8Ni_5Co_2$ and $Al_{85}Gd_8Ni_5Co_2$ alloys exhibiting the supercooled liquid region and the $Al_{85}Nd_8Ni_5Co_2$ and $Al_{85}Mm_8Ni_5Co_2$ alloys exhibiting just very beginning of the glass-transition phenomenon were chosen for the study and subjected to cold rolling with 33 % reduction. The studied alloys have close values of crystallization temperatures and crystallize by the nucleation and growth reaction.

It is found that contrary to crystallization on heating, no intermetallic compounds but only a very small volume fraction of α -Al nano particles (<1 vol.%) was formed during the deformation-induced crystallization of $Al_{85}Y_8Ni_5Co_2$ glassy and $Al_{85}Nd_8Ni_5Co_2$ amorphous alloys, while $Al_{85}Gd_8Ni_5Co_2$ and $Al_{85}Mm_8Ni_5Co_2$ samples remain fully disordered. The most important factor responsible for the suppression of precipitation of the intermetallic compounds is believed to be the effect of pressure during cold rolling as FCC structure of α -Al is supposed to have higher atomic packing density than that of the intermetallic compound ($Al_{16}Y_4Ni_4Co_3$ or $Al_{26}Nd_3Ni_3Co$) which symmetry is lower than that of the FCC lattice. The applied pressure favors precipitation of the phases with high packing density. The effect of rising temperature within the shear bands also favors crystallization and enhances diffusion-controlled growth. The higher growth rate of α -Al particles in the cold-rolled $Al_{85}Nd_8Ni_5Co_2$ amorphous alloy compared to the cold-rolled $Al_{85}Y_8Ni_5Co_2$ glassy alloy may indicate significantly higher deformation-induced diffusion rate of the alloying elements in the former alloy.

As these alloys have a nucleation and growth crystallization behavior on heating they do not exhibit significant deformation induced crystallization compared to Al-RE-Ni alloys [19-20] studied earlier which can contain pre-existing nuclei and exhibit just growth behavior.

3.3 Formation of in-situ Al-based glassy-nanocomposites upon rapid solidification

It is also found that the addition of Pd to Al-Y-Ni-Co alloys substituting Y caused disappearance of the supercooled liquid region as well as the formation of the highly dispersed primary fcc-Al nanoparticles about 3-7 nm in size homogeneously embedded in the glassy matrix upon solidification [31]. The value of the activation energy for the growth of α -Al nanocrystals of 146 kJ/mol obtained using Kissinger analysis is very close to the activation energy for self diffusion of pure Al. An extremely high density of precipitates of the order of $10^{24} m^{-3}$ is obtained (Fig. 2). This is the highest precipitation density observed so far in Al-based metallic glasses.

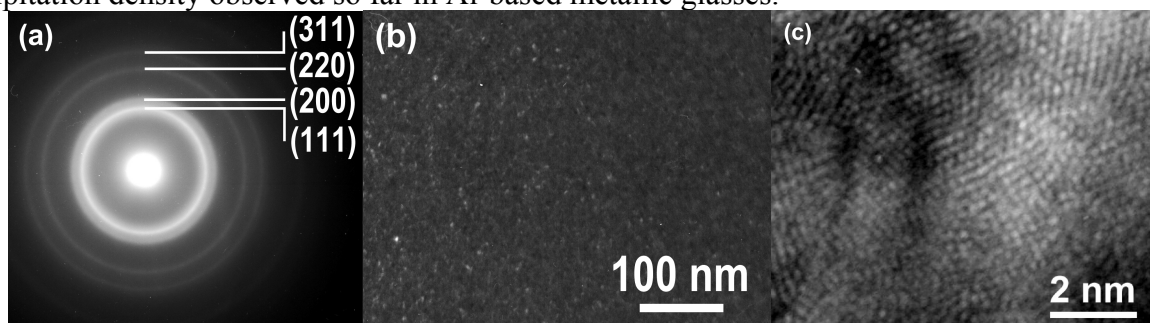


Fig. 2. (a) selected-area electron diffraction (SAED) pattern (indexing according to fcc Al) (b) TEM dark-field image and (c) HRTEM image of the as-solidified $Al_{85}Y_4Ni_5Co_2Pd_4$ alloy.

As indicated by the high-resolution TEM (HRTEM) (Fig. 2 (c)), in some areas where nuclei of α -Al nano-particles were located close enough to each other, the particles got in touch with each other upon growth and the crystal lattice of α -Al nanoparticles is heavily distorted elastically. Dislocations and other defects are observed within various α -Al nanograins (Fig. 2). In some cases these dislocations form low-angle boundaries. The broad X-ray diffraction peaks in the XRD pattern of $\text{Al}_{85}\text{Y}_4\text{Ni}_5\text{Co}_2\text{Pd}_4$ glassy alloy were fitted with Gaussian function. The resulted d-spacings for (111) and (200) are 0.2338 nm and 0.2030 nm [32], respectively, and correspond very well to that of pure Al. The broad diffraction peak from the amorphous phase contributes to the intensity of (111).

As the diffraction peaks were significantly broadened it was possible to estimate the coherent scattering area ($D_{(hkl)}$) size (crystallite size). An intrinsic broadening of the diffraction peak and the coherent scattering area D_{hkl} size are calculated according to the procedure described Ref. 33. The resulted D_{hkl} values for two strong diffraction peaks (111) and (200) are 2.5 and 3.5 nm, respectively. The latter value is more reasonable as broad diffraction peak from the residual glassy phase contributes to the intensity of (111) peak. The reason for the observed slight discrepancy between the calculated and observed particles size using (200) peak is a high degree of micro-strain within the α -Al lattice (see Fig. 2) which increases peaks breadth. It is consistent with neutron diffraction study of Al-Y-Ni alloys which indicated that Y-rich glasses are homogeneous while Ni-rich glasses have compositional inhomogeneity [34].

Compared to α -Al nanocrystals produced by the annealing of the glassy matrix which are usually found to be free of linear defects α -Al nanocrystals in the as-solidified Al-Y-Ni-Co-Pd sample contain microstrain and linear defects like dislocations. The source of the dislocations and the distortions of the crystalline lattice is believed to be impingement of the growing particles and possibly the difference in thermal expansion coefficients of crystalline Al and the multicomponent amorphous phase. Both factors lead to stresses on cooling in a solid state. The observed dislocations are attracted to the grain boundaries but did not annihilate on them owing to a high cooling rate in the order of 10^5 - 10^6 K/s during melt spinning.

The addition of Pd slightly increases the Vickers microhardness of $\text{Al}_{85}\text{Y}_8\text{Ni}_5\text{Co}_2$ alloy of HV 340 ± 15 . The harnesses of the $\text{Al}_{85}\text{Y}_6\text{Ni}_5\text{Co}_2\text{Pd}_2$ and $\text{Al}_{85}\text{Y}_4\text{Ni}_5\text{Co}_2\text{Pd}_4$ alloys are HV 350 ± 10 and HV 360 ± 15 , respectively. It indicates nearly the same level of yield strength ($\sigma_y = 9.8\text{HV}/3$) of these alloys. The Pd-bearing samples also exhibit a good bend ductility, the same as that of the $\text{Al}_{85}\text{Y}_8\text{Ni}_5\text{Co}_2$ alloy.

4. Conclusion

Al-RE-TM metallic glasses are prospective materials for different applications as structural materials due to their high strength and relatively low density. The studies of crystallisation process are important from the commercial viewpoint as precipitation of nanoscale α -Al leads to strengthening of the amorphous matrix while precipitation of the intermetallic compounds may cause embrittlement of the alloy. Crystallization of Al-based glassy and crystalline alloys is studied in a wide temperature and composition ranges. It is found that the supercooled liquid greatly influences crystallization behaviour of these metallic glasses. The rapidly solidified $\text{Al}_{85}\text{Y}_4\text{Ni}_5\text{Co}_2\text{Pd}_4$ alloy has the structure of a crystal-glassy nanocomposite, with a high density of α -Al nanocrystals which primarily precipitated on cooling from the melt and are found to be homogeneously distributed within the amorphous matrix. An extremely high number density of α -Al nanoparticles in the $\text{Al}_{85}\text{Y}_4\text{Ni}_5\text{Co}_2\text{Pd}_4$ alloy of the order of 10^{24} m^{-3} is believed to be the highest number density value obtained so far in the as-solidified Al-based glassy alloys. The Pd-bearing alloys are presumed to have nearly the same level of yield strength as the Pd-free one and exhibit as good bend ductility as the $\text{Al}_{85}\text{Y}_8\text{Ni}_5\text{Co}_2$ alloy. The direct observation of dislocations within nanoscale elastically distorted α -Al particles having an extremely small size below 7 nm which did not annihilate at room temperature is shown.

References

- [1] A. Inoue, K. Ohtera, A. P. Tsai, T. Masumoto: *Jpn. J. Appl. Phys.*, 27 (1988) 736-739.
- [2] A. Inoue, K. Ohtera, A. P. Tsai, T. Masumoto: *Jpn. J. Appl. Phys.*, 27 (1988) 280-282.
- [3] A. Inoue, K. Ohtera, A. P. Tsai, T. Masumoto: *Jpn. J. Appl. Phys.*, 27 (1988) 479-482.
- [4] G. J. Shihlet, Y. He and S. J. Poon: *J. Appl. Phys.*, 64 (1988) 6863-6865.
- [5] A. Inoue, N. Matsumoto, and T. Masumoto: *Mater. Trans. JIM* 31 (1990) 493-495.
- [6] A. Inoue, S. Sobu, D. V. Louzguine, H. Kimura, K. Sasamori: *J. Mater. Res.*, 19 (2004) 1539-1543.
- [7] A. Inoue, N. Matsumoto, T. Masumoto: *Mater. Trans. JIM*, 31 (1990) 493-495.
- [8] A. R. Yavari and D. Negri: *Nanostr. Mater.* 8 (1997) 969-986.
- [9] Y. H. Kim, A. Inoue and T. Masumoto: *Mater. Trans. JIM*, 32 (1991) 599-608.
- [10] A. Inoue: *Prog. Mater. Sci.* 43 (1998) 365-520.
- [11] M. Calin, A. Rudiger and U. Koester: *J. Metast. and Nanocryst. Mater.*, 8 (2000) 359-364.
- [12] N. Bassim, C.S. Kiminami and M.J. Kaufman: *J. Non-Cryst. Solids*, 273 (2000) 271-276.
- [13] J.H. Perepezko and R.J. Hebert: *J. Metall.* 54 (2002) 34-39.
- [14] J. H. Perepezko, R. J. Hebert and W. S. Tong: *Intermetallics* 10 (2002) 1079-1088.
- [15] J. H. Paik, F. W. J. Botta, and A. R. Yavari: *Mater. Sci. Forum* 305 (1996) 225-227.
- [16] A. R. Yavari, W. J. Botta, C.A.D. Rodrigues, C. Cardoso, and R.Z. Valiev: *Scr. Mater.*, 46 (2002) 711-716.
- [17] D. V. Louzguine, A. Inoue: *J. Light Met.* 1 (2001) 105-109.
- [18] R. D. Sá Lisboa, C. S. Kiminami: *J. Non-Cryst. Solids*, 304 (2002) 36-43.
- [19] K. Hono, Y. Zhang, A. P. Tsai, A. Inoue, T. Sakurai: *Scripta Mater.* 32 (1995) 191-196.
- [20] H. Chen, Y. He, G. J. Shiflet, and S. J. Poon: *Nature* 367 (1994) 541-543.
- [21] W. H. Jiang, F. E. Pinkerton, and M. Atzmon: *J. Appl. Phys.* 93 (2003) 9287-9290.
- [22] W. H. Jiang and M. Atzmon: *Acta Mater.* 51 (2003) 4095-4105.
- [23] J. W. Christian: *The Theory of Transformations in Metals and Alloys*, Pergamon Press Ltd., Oxford, 1975, p. 369-586.
- [24] R. D. Sá Lisboa, C. Bolfarini, W. J. Botta F. and C. S. Kiminami: *Appl. Phys. Lett.*, 86 (2005) 211904-211906.
- [25] T. Egami, Y. Waseda: *J. Non-Crystall. Sol.* 64 (1984) 113-134.
- [26] D. V. Louzguine and A. Inoue: *Appl. Phys. Lett.*, 79 (2001) 3410-3413.
- [27] D. V. Louzguine-Luzgin, A. Inoue and W. J. Botta: *Appl. Phys. Lett.* 88 (2006) 011911-011913.
- [28] A. Inoue: *Mater. Trans. JIM* 36 (1995) 866-875.
- [29] W. F. Gale, T. C. Totemeier, editors. *Smithells Metals Reference Book 8-th Edition* (Elsevier Burlington 2004), p 4-44.
- [30] D. V. Louzguine-Luzgin and A. Inoue: *J. Non-Cryst. Sol.* 352 (2006) 3903-3909.
- [31] D. V. Louzguine-Luzgin and A. Inoue: *J. Alloys and Comp.* 399 (2005) 78-85.
- [32] D. V. Louzguine-Luzgin and A. Inoue: *J. Mater. Res.*, 21 (2006) 1347-1350.
- [33] S. S. Gorelik, U. A. Skakov and L. N. Rastorguev: *X-ray and Electron-optic Analysis*. (MISIS, Moscow, 1994), p. 328-330.
- [34] Z. Altounian, S. Saini, J. Mainville and R. Bellissent: *Physica B: Condensed Matter*, 241-243 (1997) 915-917.